XI International Conference on Computational Plasticity. Fundamentals and Applications
COMPLAS XI
E. Oñate, D.R.J. Owen, D. Peric and B. Suárez (Eds)

ON THE PERFORMANCES OF DIFFERENT NODAL INTEGRATION TECHNIQUES AND THEIR STABILIZATION

F.GRECO[*], L.FILICE[*], I.ALFARO[†] AND E.CUETO[†]

[*] Dept. of Mechanical Engineering, University of Calabria, Italy
e-mail: francesco.greco@unical.it
l.filice@unical.it

[†] Aragon Institute of Engineering Research, Universidad de Zaragoza, Spain
e-mail: iciar@unizar.es
ecueto@unizar.es

Key words: Nodal Integration, stabilization.
Abstract. Finite element method was successfully applied in the simulation of several forming processes; however, it does not represent an absolute reference point. In fact, large deformation corresponds to a heavy mesh distortion. Powerful rezoning-remeshing algorithms strongly reduce the effects of such a limitation but the computational time significantly increases and additional errors occur. Nodal Integration is a recently introduced technique that allows finite element method to provide reliable results also when meshes becomes distorted in traditional FEMs. Furthermore, volumetric locking problems seem to be avoided using this integration technique instead of other methods such as coupled formulations. Nevertheless, spurious low-energy modes appear due to the nodal averaging of strain. For this reason stabilizing methods application seems to be suitable. What is more, different nodal integration techniques have been proposed, although spurious modes are a common problem. In this paper the performances of three different nodal integration techniques and the effects of a recently introduced stabilization methodology are studied simulating a classical forming process.

1 INTRODUCTION

Finite element method is surely the referential numerical technique in the analysis of solid mechanics problems. It has been successfully used in the simulation of several phenomena, providing excellent results.

Nevertheless, FEM requires an adequate discretization of the computational domain in terms of node and elements since the final results are sensible to the distribution and regularity of this decomposition [1]. In small deformation problems, such as linear elasticity, it is quite easy to obtain a reliable discretization and very accurate solutions, also with a low computational cost. The situation suddenly changes in problems characterised by large deformations, such as the material forming processes. In this case, if a Lagrangian formulation is used, the mesh moves with material and elements become so distorted that numerical results lose their validity.

Different techniques have been developed across the last years to overcome this problem.

Among them, Eulerian formulations, arbitrary Lagrangian-Eulerian (ALE) and remeshing techniques are the most known. In any case, additional drawbacks appeared especially when the remeshing techniques are applied. Remeshing-rezoning approach avoids the results worsening but, at the same time, the computational time increases and supplementary errors are introduced.

A possible alternative is the use of meshless methods [2] but in many cases the improvement of the results quality, with the same number of degrees of freedom, is vanished by the very high computational time for the shape functions calculation.

In the FEM environment the performances of the analysis depend on the used element. The constant strain elements (triangle with 3 nodes or tetrahedrons with 4 nodes in the 3D case) would be preferable for different reasons, especially when non-linear problems are investigated. Nevertheless their poor performances force the researchers to use high-order elements, such as 8 nodes tetrahedral or hexahedral. However, these formulations are not free from the results worsening due to the mesh deterioration and, besides, the remeshing procedure is very costly to be implemented, particularly for the hexahedral elements.

A great drawback of conforming FEM is that the numerical model is always more stiff than the studied material. What is more, any mesh distortion gives a further spurious stiffness to the model. Introducing a Nodal Integration scheme the FEM model is not necessarily stiffer than the real material; on the contrary, in many applications the initial model is less stiff and a distorted mesh could paradoxically have a beneficial effect on the performances.

The basics of nodal integration in FE analysis were firstly introduced by Dohrmann et al. [3]. They showed that applying the new technique the performances of the constant strain elements are significantly improved in the study of acute bending problems. Moreover the method was shown to be free from volumetric locking in the simulation of quasi-incompressible materials.

The nodal integration (NI) has been introduced also in the meshless environment [4-5], as an alternative to the standard integration, due to its efficiency and applicability in large deformations problems.

Puso and Solberg [6] noted that the formulation proposed in [3] was prone to spurious low energy modes and introduced a new stabilized nodal integrated tetrahedral element. They also analytically showed that their new element was stable and consistent for linear elasticity.

In [7] the stabilizing technique proposed in [6] was further analyzed and extended to the meshless methods, since spurious modes were detected also in this case.

In this work a comparison was done between the two nodal integration schemes proposed in [3] and the scheme proposed in [4], whose usage is suitable also in the FEM. The three techniques will be applied to the simulation of extrusion, as a typical example of a forming process where significant deformations are present.

Moreover the effect of the stabilization technique presented in [6] was studied.

2 THE NODAL INTEGRATION FORMULTIONS

Let Ω be a 2D computational domain, discretized by a cloud of nodes, from 1 to N_N denoted by I and a mesh of triangular elements, from 1 to N_E, denoted by J. In a traditional finite element code, the strain is calculated using the gradient matrix $\boldsymbol{B}$, that, if $\varphi_1, \varphi_2 \ldots . \varphi_{N_N}$ are the shape functions, is defined as:

$$\boldsymbol{B} = \begin{bmatrix} \frac{\partial \varphi_1}{\partial x} & 0 & \cdots & \frac{\partial \varphi_{N_N}}{\partial x} & 0 \\ 0 & \frac{\partial \varphi_1}{\partial y} & \cdots & 0 & \frac{\partial \varphi_{N_N}}{\partial y} \\ \frac{\partial \varphi_1}{\partial y} & \frac{\partial \varphi_1}{\partial x} & \cdots & \frac{\partial \varphi_{N_N}}{\partial y} & \frac{\partial \varphi_{N_N}}{\partial x} \end{bmatrix} \tag{1}$$

Thus, if $\boldsymbol{d}$ is the vector containing the (unknown) nodal displacements, the strain is given by:

$$\boldsymbol{\varepsilon}(\boldsymbol{x}) = \boldsymbol{B}(\boldsymbol{x})\boldsymbol{d} \tag{2}$$

If three-node triangular elements are used, the shape functions derivates are constant in every element, and also the matrix $\boldsymbol{B}$. Thus element strain could be expressed as:

$$\boldsymbol{\varepsilon}_J = \boldsymbol{B}_J \boldsymbol{d} \tag{3}$$

and, if $\boldsymbol{E}$ is the matrix that relates strain and stress vectors, a stiffness matrix $\boldsymbol{K}$ is assembled, in order to solve the approximated problem:

$$\boldsymbol{K} = \int_{\Omega} \boldsymbol{B}^T \boldsymbol{E} \boldsymbol{B} d\Omega = \sum_{J=1}^{N_E} \boldsymbol{B}_J^T \boldsymbol{E} \boldsymbol{B}_J \times A_J \tag{4}$$

Where A_J is the area of each element.

When the nodal integration is applied to FEM a constant strain field $\tilde{\boldsymbol{\varepsilon}}_I$ is assumed within a particular volume $\tilde{V}_I$, associated to each node.

The easiest to interpret NI scheme is the one proposed in [4], that is based on the Voronoi diagram [8]. As it is shown in Figure 1, the Voronoi diagram is a subdivision of the computational domain in regions Ω_I, where each region is associated with a node I, so that any point in Ω_I is closer to the node I than to any other node in the domain.

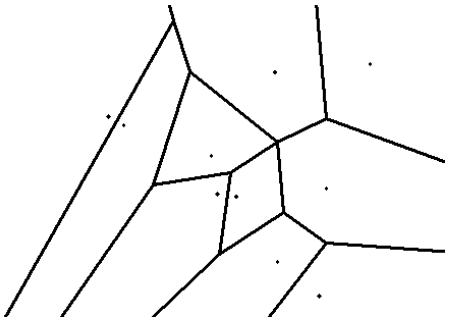

Figure 1: An example of Voronoi Diagram

In this case the nodal volume $\tilde{V}_I$ is, for each node, the area A_I of the corresponding cell in the diagram and the assumed strain is the average strain in this cell:

$$\tilde{\boldsymbol{\varepsilon}}_I = \frac{1}{A_I} \int_{\Omega_I} \boldsymbol{\varepsilon}(\boldsymbol{x}) d\Omega \tag{5}$$

Since constant strain elements are used, equation 5 could be rewritten as:

$$\tilde{\boldsymbol{\varepsilon}}_I = \frac{1}{A_I}\sum_{J=1}^{N_E} \boldsymbol{\varepsilon}_J \times Area(\Omega_I \cap T_J) \tag{6}$$

We will call this scheme Global Voronoi Integration (GV). Observing that $\sum_{J=1}^{N_E} Area(\Omega_I \cap T_J) = A_I$, the strain $\tilde{\boldsymbol{\varepsilon}}_I$ is a weighted average of the strain of the elements. The two NI schemes proposed in [3] provide also a strain averaging, but the weights are different. In particular it is imposed that the strain $\tilde{\boldsymbol{\varepsilon}}_I$ depends only on the strain of the set of elements S_I that contain the node I. According to this constraint, one of the two schemes is also based on the Voronoi Diagram, but in this case the Diagram is locally calculated in each triangle. In particular each triangle T_J is divided in three zones t_{JI}, associated to its nodes, so that every point in t_{JI} is closer to the node I than to any other node in T_J. Then the nodal volume and the assumed strain are calculated as:

$$\tilde{V}_I = \sum_{J\in S_I} Area(t_{JI}) \tag{7}$$

$$\tilde{\boldsymbol{\varepsilon}}_I = \frac{1}{\tilde{V}_I}\sum_{J\in S_I} \boldsymbol{\varepsilon}_J \times Area(\, t_{JI}) \tag{8}$$

We will refer to this scheme as Local Voronoi Integration (LV). The other technique proposed in [3] is not based on geometrical considerations but provides a heuristic calculation of the assumed strain, imposing that the area of the triangles is divided in three equal parts, associated to its nodes. Hence:

$$\tilde{V}_I = \sum_{J\in S_I} \frac{Area(T_J)}{3} \tag{9}$$

$$\tilde{\boldsymbol{\varepsilon}}_I = \frac{1}{\tilde{V}_I}\sum_{J\in S_I} \boldsymbol{\varepsilon}_J \times \frac{Area(T_J)}{3} \tag{10}$$

The latter scheme is called Direct Averaging Integration (DA).

3 IMPLEMENTATION OF THE METHOD AND COMPUTATIONAL TIMES

Similarly to a traditional FE interpolation the assumed strain could be related to the displacement field using an equivalent gradient matrix:

$$\boldsymbol{\varepsilon}_I = \widetilde{\boldsymbol{B}}_I \boldsymbol{d} \tag{11}$$

It is easy to demonstrate that the matrixes $\widetilde{\boldsymbol{B}}_I$ will be a weighted average of the element matrixes $\boldsymbol{B}_J$, calculated using the same weight coefficients of the strain case, depending on the specific NI scheme. Thus, in the implementation of the method, the matrixes $\widetilde{\boldsymbol{B}}_I$ are calculated and the global stiffness matrix is assembled as:

$$\widetilde{\boldsymbol{K}} = \sum_{I=1}^{N_N} \widetilde{\boldsymbol{B}}_I^T \boldsymbol{E} \widetilde{\boldsymbol{B}}_I \times \tilde{V}_I \tag{12}$$

This last calculation takes an additional computational time that is negligible respect to a traditional FEM code when DA scheme is used. In fact, only the volume of the elements has to be calculated and the equivalent gradient matrixes are directly calculated as a linear combination of the element gradient matrixes.

The situation changes in the Voronoi-based (GV and LV) techniques. In particular in the GV case all the areas of the intersections between a given Voronoi cell and the elements have to be calculated. In this work this operation has been carried out describing both the cells and the elements as convex polygons and then applying the Lasserre algorithm [9]. Although the computational complexity is linear with the number of nodes this is a significant time consuming operation that could take a computational time of the same order or slightly higher than the total time consumed for the analysis by a traditional FEM code. Anyway, the asymptotical linear complexity ensures that for clouds composed by a high enough number of nodes this time tends to be smaller than the time requested for the resolution of the equations.

The LV scheme could be also implemented describing the geometrical entities by convex inequalities and applying the Lasserre algorithm or other similar. Nevertheless in order to advantage the rapidity of the simulation other more efficient strategies are possible. In particular, after determining the coordinates of the circumcenters of the triangular elements, the intersections areas could be find out calculating the areas of particular triangles. This operation takes a practically negligible time, as in the DA case.

Concerning the computational times of a NI code two more aspects have to be taken into account. The first is that the assembled stuffiness matrix is denser that the matrix that would be assembled using a traditional procedure. This increases the resolution time about the 30%.

On the contrary the second aspect advantages the new technique. In fact the use of Nodal Integration seems to avoid the volumetric locking problems typical of FEM when incompressibility is imposed. Thus, unlike in a traditional code where coupled pressure-velocity formulations has to be used to overcome to this problem, only the velocities could be taken as unknowns, reducing significantly the resolution time. This second recovery offsets the precedent augment.

4 THE CASE STUDY

According to the introduction, an extrusion process has been analyzed as a typical example of forming process in which the large deformation stresses the classical FE formulation. A plain strain 2D model has been used, with the geometrical characteristics and the boundary conditions illustrated in figure 2. As far as the material behavior is considered, in the forming processes and in particular in extrusion, strains are very large as compared to elastic ones. Thus, it is a common practice for this kind of processes to assimilate the material behavior to a viscoplastic one, in which the stress depends on the strain rate [10].

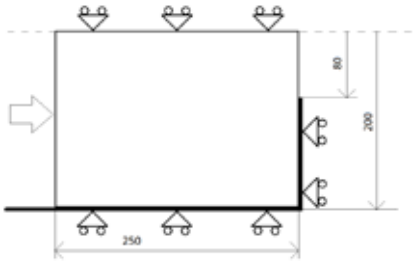

Figure 2: Sketch of the used model

In particular, a Northon-Hoff model has been used; it relates the effective stress to the equivalent strain rate in the following form:

$$S_f = C\bar{\dot{\varepsilon}}^n \tag{13}$$

Together with this global relation the stress components assembled in the vector $\boldsymbol{\sigma} = |\sigma_x \quad \sigma_y \quad \tau_{xy}|^T$ has to be related to the strain rate components, $\dot{\boldsymbol{\varepsilon}} = |\dot{\varepsilon}_x \quad \dot{\varepsilon}_y \quad \dot{\gamma}_{xy}|^T$. In the used model this corresponds to define a viscosity μ in the following form:

$$\mu = \frac{C}{3}\bar{\dot{\varepsilon}}^{n-1} = \mu_0\bar{\dot{\varepsilon}}^{n-1} \tag{14}$$

and to use it in the assembling of the constitutive matrix $\boldsymbol{E}$, whose expression, in plain strain, is given by:

$$\boldsymbol{E} = \frac{2\mu}{1-2\nu}\begin{vmatrix} 1-\nu & \nu & 0 \\ \nu & 1-\nu & 0 \\ 0 & 0 & \dfrac{1-2\nu}{2} \end{vmatrix} \tag{15}$$

In this work a value of the Poisson's coefficient $\nu = 0.49999$ has been employed in order to impose incompressibility.

The used values of the Northon-Hoff coefficients have been:

$$\mu_0 = 150, \qquad n = 0.2 \tag{16}$$

that, according to [11], correspond to some common Aluminum alloys.

Due to the non-linear character of the constitutive equations an iterative scheme has to be applied for their resolution. In particular, taking into account the strong nonlinearities given from the value of n, the Direct Iteration Method [12] has been preferred to the Newton-Raphson scheme, whose convergence is not ever straightforward in this type of problems. This iterative procedure has been combined with the stabilization technique, as it is discussed in the following chapter.

5 THE STABILIZATION TECHNIQUE

According to [6], a stabilized stiffness matrix $\boldsymbol{K_{STAB}}$ has to be assembled using the stabilization parameter α and the modified behavior matrix $\widetilde{\boldsymbol{E}}$ that, when a linear problem is studied, leads to:

$$\boldsymbol{K_{STAB}} = \boldsymbol{K_{NOD}} + \boldsymbol{K_{ELEM}} = \sum_{I=1}^{N_N} \widetilde{\boldsymbol{B}}_I^T (\boldsymbol{E} - \alpha \widetilde{\boldsymbol{E}}) \widetilde{\boldsymbol{B}}_I \tilde{V}_I + \alpha \sum_{J=1}^{N_E} \boldsymbol{B}_J^T \widetilde{\boldsymbol{E}} \boldsymbol{B}_J A_J \tag{17}$$

The influence of α on the results will be discussed in the relative section; the matrix $\widetilde{\boldsymbol{E}}$ differs from $\boldsymbol{E}$ because it is assembled using a different Poisson's coefficient, since locking problems would be present in the elementary term. A value of $\tilde{\nu} = 0.4$ has been used.

In the resolution of the non-linear equations the stabilized stiffness matrix is then assembled in the form:

$$\boldsymbol{K}_{\boldsymbol{STAB}}^{n} = \sum_{I=1}^{N_N} \widetilde{\boldsymbol{B}}_I^T [\boldsymbol{E}_{(\mu^{n-1})} - \alpha \widetilde{\boldsymbol{E}}_{(\mu^{n-1})}] \widetilde{\boldsymbol{B}}_I \tilde{V}_I + \alpha \sum_{J=1}^{N_E} \boldsymbol{B}_J^T \widetilde{\boldsymbol{E}}_{(\mu^{n-1})} \boldsymbol{B}_J A_J \tag{18}$$

where the superscript n indicates the iteration within a time increment as well as μ^{n-1} is the viscosity calculated from the previous velocity field. The iteration method is initialized with $\mu = \mu_0$ and obviously terminates when $\boldsymbol{v}^n = \boldsymbol{v}^{n-1}$. Obtained the velocity values the geometry is updated and the following time step could be studied.

6 RESULTS

The investigated process was simulated using a punch speed $v_p = 1mm/s$ and considering 50 time steps ($1s/step$). In figure 3 are reported the pressure and velocity field, using the LV scheme, with a regular mesh and an irregular one of about 1000 nodes. No stabilization has been considered. Looking at the velocity field of the regular mesh the presence of the spurious modes is clearly observable; what it is more the pressure field is completely wrong since it presents strong oscillation in the direction of the mesh. The situation is quite different when the irregular mesh is used; in this case the velocity field is quite more regular as well as the pressure field has a satisfactory trend, considering the reduced number of nodes. This confirms the well-known phenomenon that the regularity of the mesh favors the spurious deformations.

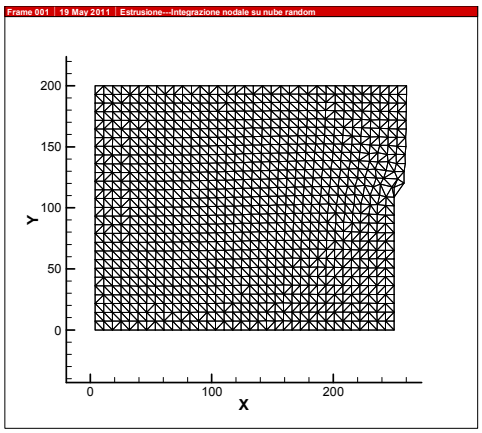

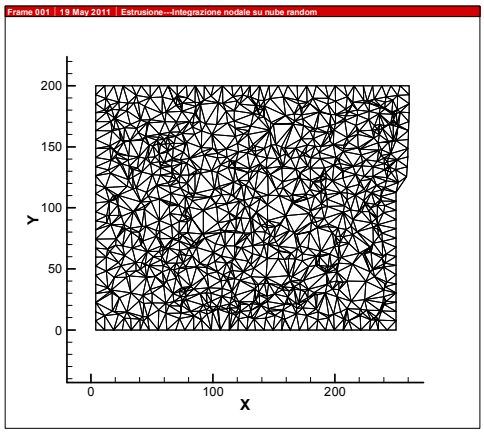

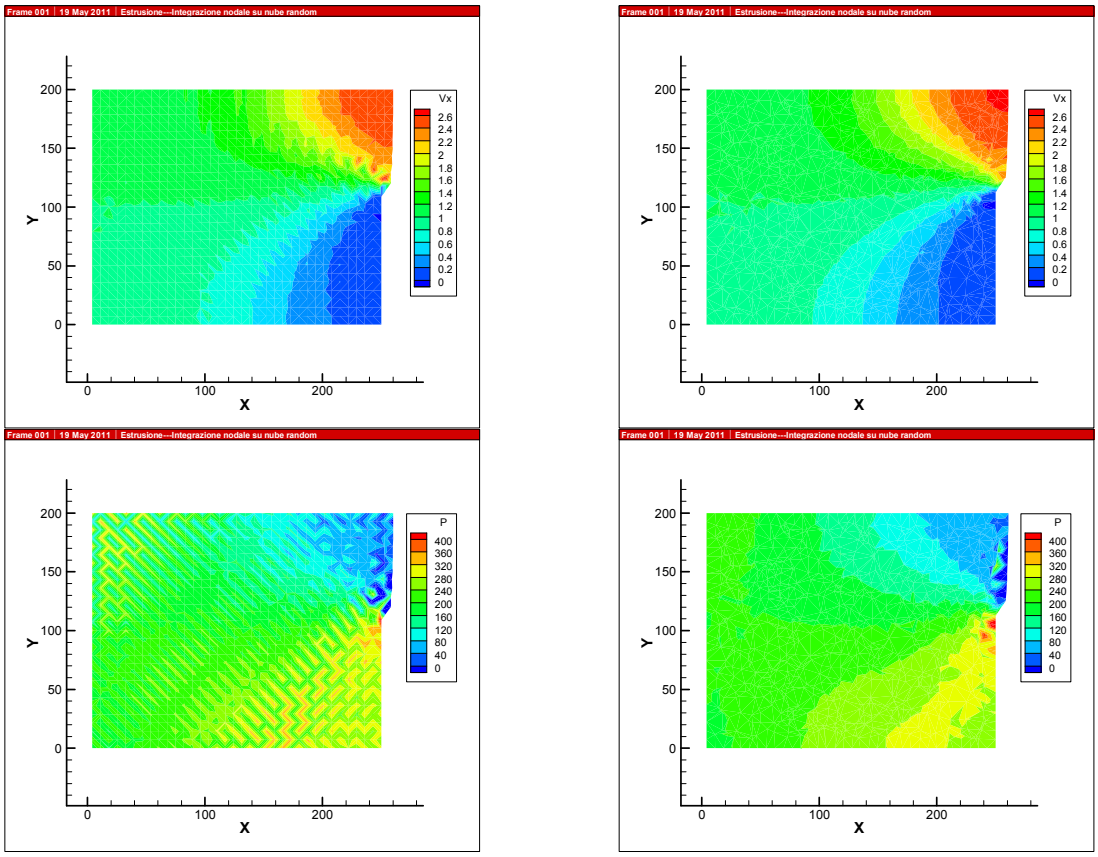

Figure 3: The regular and the irregular mesh and their respective pressure and velocity fieldsp

Since a first stabilizing effect is given only by using an irregular mesh the three NI schemes has been preliminarily compared without introduce the stabilization technique, but using only the benefic effects of the irregularity of the mesh.

In figure 4 has been reported the punch load during the process predicted with the three techniques, using two meshes, of 2000 and 5000 nodes respectively.

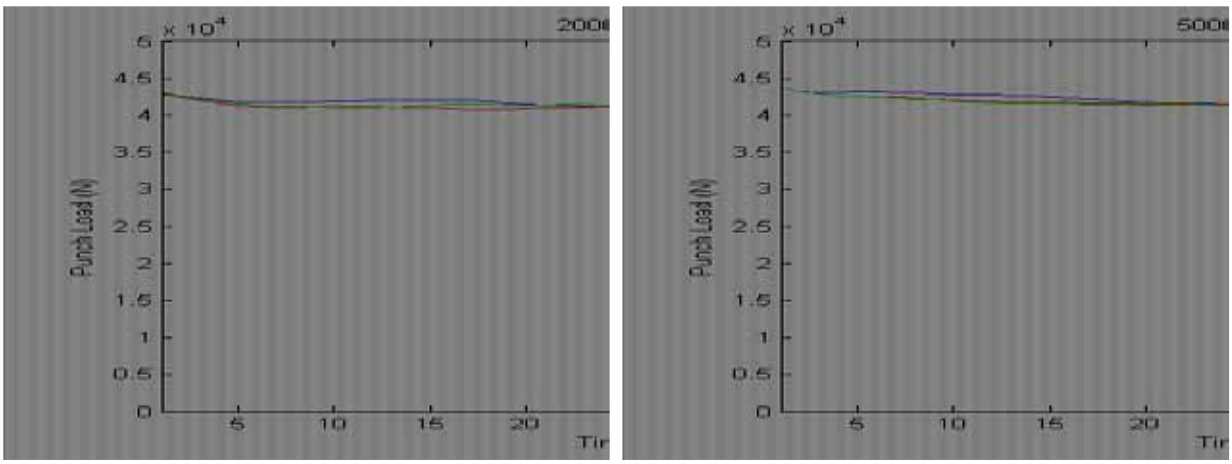

Figure 4: Extrusion load for the three scemes with different types of mesh

Looking at the graphs a very slightly difference is observed between the different schemes. Anyway the extrusion force is a global variable whose prevision does not heavily depends on local phenomena that could condition the specific code prediction; for this reason a better comparison could be done looking at the flow stress distribution at the last step, in figure 4.

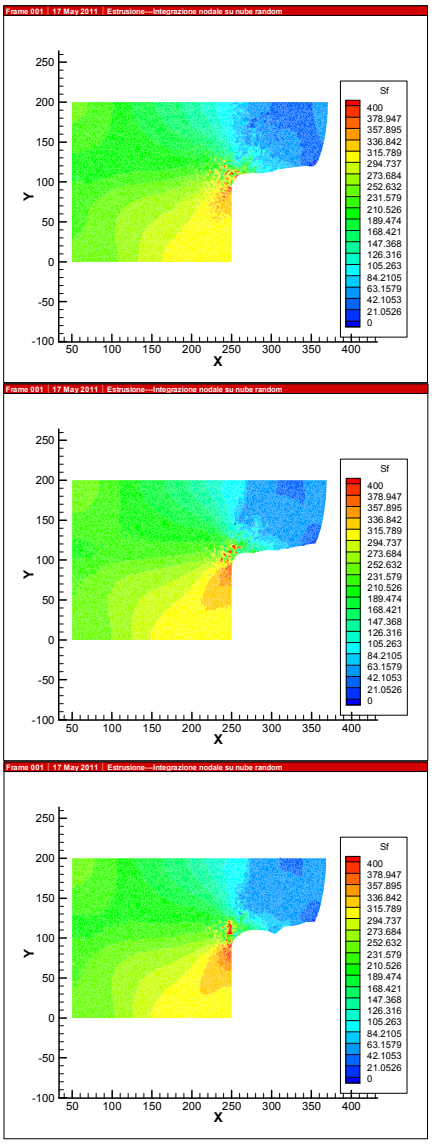

Figure 5: The flow stress distribution for the three nodal integration schemes

In this case the Voronoi-based schemes are quite similar, while the DA presents a slightly lower and more irregular field. Since, according to session 3, the DA and LV schemes would be preferable for the computational times and considering the more regular trend of LV results, that are in excellent agreement with GV ones, the Local Voronoi integration scheme appears to be the most convenient choice.

Concerning the stabilization in figure 6 the velocity field at the 4th step is reported for the two types of mesh (again using the LV scheme with 1000 nodes) and for different values of α.

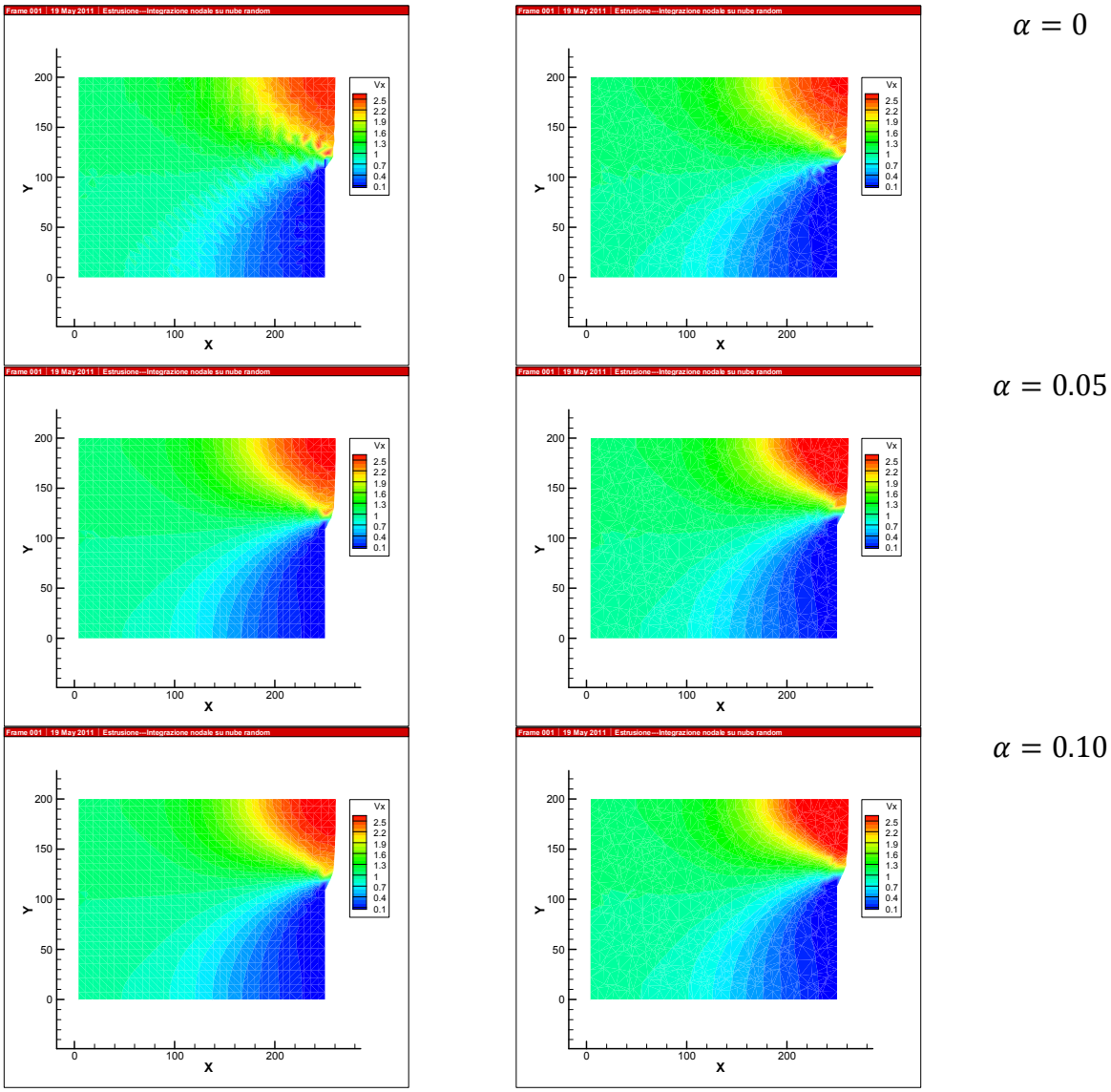

Figure 6: Influence of the stabilization parameter on the velocity field, for the regular mesh (left) and the irregular one (right)

It is very interesting to note that already a value of $\alpha = 0.05$ has a significant stabilizing effect and that imposing $\alpha = 0.10$ even the regular mesh simulation has a very regular velocity field, as in a traditional FEM.

Even more interesting are the effects of α on the punch load. In order to compare the prediction capabilities of the NI techniques with a reference result, the investigated case study has been also simulated with the commercial FEM code DEFORM, that demonstrated in the last years an excellent accuracy in 2D models such as the one considered in this work; moreover, a very refined mesh has been used in this simulation so that the DEFORM solution

could be considered to be very close to the analytical one. Observing the figure 7, obtained for the LV scheme with an irregular mesh of 5000 nodes, two evidences are remarkable:

- all the stabilized curves are close to the DEFORM solution, while the non-stabilized one presents a significant lower load prediction.
- increasing the value of α the stabilized curves cover a range that includes the DEFORM and presumably also the effective solution.

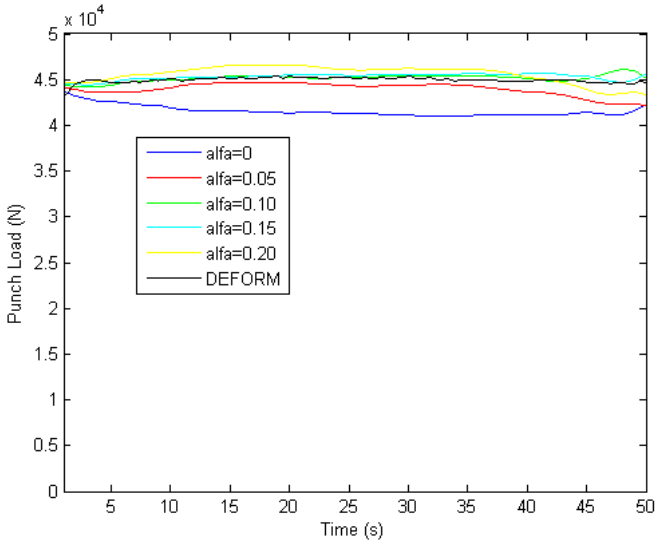

Figure 7: Punch load for different values of the stabilization parameter

The first aspect is due to the more irregular velocity field that leads to a different shape of the extruded material. In figure 8 a comparison is done between the shape of the non-stabilized simulation and stabilized one with α=0.10.

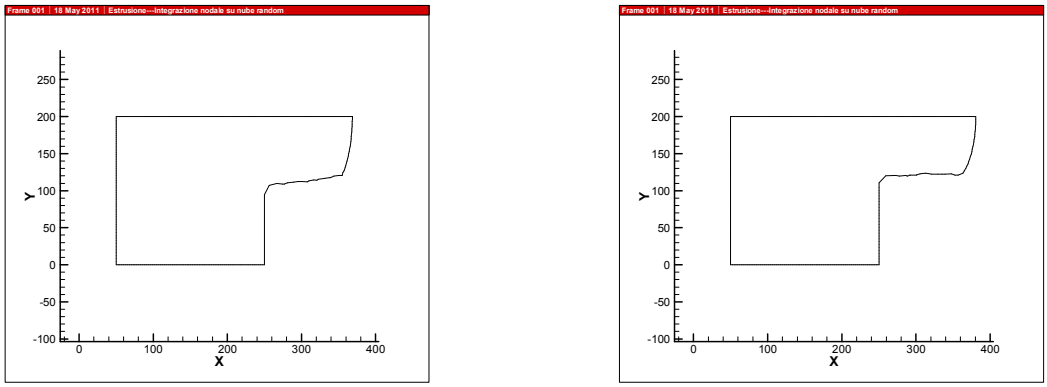

Figure 5: The predicted shape for the non-stabilized code (left) and the stabilized (right)

In particular, when the stabilization is not applied, the extruded material has a larger shape and, for this reason, the requested load results to be slower.

Concerning the second consideration, the influence of α on the load could be explained observing that the traditional FEM matrix $\boldsymbol{K_{ELEM}}$ in equation 17 gives additional stiffness to the model with the increase of α. Analyzing the curves in figure the optimal value of α, in this

application, is about 0.10. Anyway, in general, the most favorable choice of its value depends on several aspects, such as the mesh characteristics, and could be also a lower value, since as it has been shown it is already sufficient to stabilize the model.

7 CONCLUSIONS

In this paper three nodal integration techniques have been compared in the simulation of an extrusion process. The Voronoi-based formulations have shown a slightly better quality of predictions; in particular the LV scheme appears to be the most favorable choice since it requires only a negligible computational time for the geometrical part.

Furthermore the stabilization of this method has been discussed. In particular it has been shown that even if satisfactory results are obtainable using an irregular mesh, their quality is significantly improved if a stabilization is introduced; moreover varying the stabilization parameter the stiffness of the model can be properly tuned.

REFERENCES

[1] Babuška, I. and Aziz A. On the angle condition in the Finite Element Method. *SIAM Journal of Numerical Analysis* (1976) **13**:214-227.

[2] Belytschko, T., Krongauz, Y., Organ, D. and Krysl, P. Meshless Methods: An Overview and recent developments. *Computer Methods in Applied Mechanics and Engineering* (1996) **139(1-4)**:3-47.

[3] Dohrmann, C.R., Heinstein, M.W., Jung, J., Key, S.W. and Witkowski, W.R. Node-based uniform strain elements for three-node triangular and four-node tetrahedral meshes. *International Journal for Numerical Methods in Engineering* (2000) **47**:1549–1568.

[4] Jiun-Shyan Chen, Cheng-Tang Wu, Sangpil Yoon and Yang You. A stabilized conforming nodal integration for Galerkin mesh-free methods. *International Journal for Numerical Methods in Engineering* (2001) **50(2)**:435-466.

[5] Beissel, S. and Belytschko, T. Nodal Integration of the element-free Galerkin method. *Computer Methods in Applied Mechanics and Engineering* (1996) **139**:49-74.

[6] Puso, M.A. and Solberg, J. A stabilized nodally integrated tethaedral. *International Journal for Numerical Methods in Engineering* (2006) **67**:841-867.

[7] Puso, M.A., Chen, J.S., Zywicz, E. and Elmer, W. Meshfeee and finite elements nodal integration methods. *International Journal for Numerical Methods in Engineering* (2007) **74**:416-446.

[8] Preparata, F.P. and Shamos, MI. *Computational Geometry: An Introduction* (1985). Springer: New York.

[9] Lasserre, J.B. An analytical expression and an algorithm for the volume of a convex polyhedron. Optimization Theory Application (1983) **39**:363-377.

[10] Zienkiewicz, O.C. and Godbolet, P.N. Flow of plastic and visco-plastic solids with special reference to extrusion and forming processes. *International Journal for Numerical Methods in Engineering* (1974) **8**:3–16.

[11] Kalpakjian, S. and Schmid, S.R. *Manufacturing processes for engineering materials. IV Ed* (2003). Pearson Education, Inc.

[12] Kobayashi, S., Soo-ik Oh and Altan, T. *Metal forming and the finite element method* (1989). Oxford University press.